SYNTHESIS AND PROPERTIES OF THE MFI ZINCOSILICALITE

Girolamo GIORDANO[a1], Andrea KATOVIČ[a2], Ewa SZYMKOWIAK-JANISZEWSKA[b1] and Stanisław KOWALAK[b2,*]

[a] *University of Calabria, Department of Chemical Engineering and Materials, 87030 Rende, Italy; e-mail: [1] ggiorda@unical.it, [2] katovic@unical.it*

[b] *Faculty of Chemistry, A. Mickiewicz University, Grunwaldzka 6, 60-780 Poznań, Poland; e-mail: [1] eszym@amu.edu.pl, [2] skowalak@amu.edu.pl*

Received August 20, 2002
Accepted December 17, 2002

Zincosilicalite MFI with various zinc contents (up to Zn/Si = 0.07) has been synthesized by hydrothermal crystallization. The samples with the Zn/Si ratio in the range 0.03–0.07 still show the crystalline structure of MFI, but they are less ordered and differ in properties from those with lower Zn contents. The mixtures with the Zn/Si ratios higher than 0.07 resulted in amorphous products or condensed crystalline phases (quartz). The introduction of Zn affected both the crystallization time and properties of the resulting products. Usually the higher Zn/Si ratio of the gel required a longer crystallization time. The zinc introduced affected the thermal template removal making it more difficult than for the zinc-free silicalite. The obtained zincosilicates were modified by ion-exchange with various cations. Contrary to zinc-free silicalite-1, they showed considerable catalytic activity in propan-2-ol decomposition and in cumene cracking. The activity usually increased with the Zn content up to the ratio Zn/Si = 0.03 and then decreased with rising Zn loading. It also depended on the cation introduced. The Cu-modifications resulted in dehydrogenation of propan-2-ol.

Keywords: Zincosilicates; MFI; Thermal analysis; Catalytic properties; Molecular sieves; Zeolites; Heterogeneous catalysis; Hydrothermal crystallization; Cracking.

The isomorphous substitution of the lattice atoms in the crystalline molecular sieves has become a powerful method for synthesis and modification of novel materials which can be used as tailored catalysts for selected reactions. Nowadays several dozens of elements are employed as lattice components of molecular sieves. Chemical composition considerably affects stability and properties of the resulting products. Sometimes novel structures are obtained. Zinc has been reported as a component of various molecular sieves such as zincophosphates, zincoarsenates[1–4], zincoaluminosilicates[5–7], zincosilicates[8–12], zincoaluminophosphates[13]. In some cases crystalline analogs of zeolite structures have been obtained under unusually mild conditions and crystallization occurred almost spontaneously on mix-

ing the substrate solutions[1] or even on grinding the substrates[14]. The resulting zincophosphates and zincoarsenates, however, were unstable and usually decomposed above 200 °C. The reported zincosilicates were more stable, although most novel structures showed a narrow pore system[8–12] which was not suitable for catalysis and adsorption. The MFI structure (zeolites ZSM-5) has been very often used as catalyst. Besides the efficiency of active sites (mainly strong-acid sites), the medium size of the channels provides the shape selectivity effect for the reactions of commercial importance. Therefore, this structure is also interesting to be attained for the zincosilicate molecular sieves. Due to the double negative charge of the lattice zinc tetrahedra, they could be modified with various cations including protons and they might be considered as catalysts for various reactions. Moreover, some redox activity could result from the presence of zinc in the lattice. The zinc-modified zeolites MFI have been applied as active catalysts in the Cyclar process[6,7,15,16], which consists in formation of aromatics from light paraffins. The catalysts used in methanol synthesis contain mostly zinc and copper oxides[17]; it is conceivable that MFI zincosilicate modified with copper cations could be efficient for this reaction. The well-ordered crystalline structure as well as the uniform pore system could be advantageous for the catalyst performance. The attempts to synthesize aluminosilicate MFI with some admixture of zinc[6,18–20] as well as zincosilicate[12,21] have been reported. We have prepared several series of MFI zincosilicate with various zinc loading[22–25] and noticed a significant influence of the introduced zinc on properties of the resulting products. Among others we noticed that thermal removal of the template becomes more difficult for the zinc-rich samples. The aim of this work is to study the correlation between the zinc loading and properties of the resulting zincosilicate MFI. Special attention has been paid to thermal properties of the prepared samples.

EXPERIMENTAL

The zincosilicate of MFI structure has been synthesized according to conventional recipes[26]. The main difference consisted of using $Zn(NO_3)_2$ instead of aluminium compounds. Another modification comprised the use of phosphoric acid as a crystallization promoter[27]. The initial gel was formed by mixing a NaOH (Carlo Erba) solution with tetrapropylammonium bromide (TPAB) (98%, Fluka) and precipitated silica gel (BDH, Laboratory reagent) followed by adding solutions of $Zn(NO_3)_2 \cdot 6H_2O$ (Carlo Erba) and H_3PO_4 (85%, Fluka). pH of the initial gel was always ≈11, which was adjusted using H_3PO_4. The Zn/Si ratio of the initial mixtures varied in the range of 0.01–0.1. The gel crystallized at 170 °C in a Teflon lined autoclave for various periods of time (23–140 h). The synthesis was quenched every day and small samples were taken for XRD analysis to follow the progress in crystallization. The hydrothermal syntheses were stopped when the intensity of the XRD reflections of the prod-

ucts attained the maximum and did not increase any longer. The intensities of respective XRD reflections were compared with those of zinc-free silicalite. The resulting products were washed with water, dried and eventually calcined in air at 450 °C in order to remove the organic template. The details of the preparation are given in Table I. The samples after calcination were modified with Cu^{2+} and NH_4^+ cations. The ion-exchange procedure was conducted at 50 °C. Aqueous solutions (0.5 M) of NH_4Cl and of $CuCl_2$, respectively, were added (15 ml per 1 g of the sample) and the mixture was magnetically stirred for 16 h. The procedure was repeated three times with fresh aliquots of solutions and then the samples were washed and dried. The samples modified with copper were blue. The ammonium-exchanged samples were calcined at 450 °C to obtain the H-form.

The samples were characterized by standard methods such as XRD (Philips 1730/70), FTIR (KBr, Bruker Vector 22), Raman spectroscopy (FTIR Raman Nicolet 760 with Nd YAG beam), scanning electron microscopy (Philips SEM 515), elemental analysis (Shimadzu AA-660), ^{29}Si MAS NMR (Bruker MSL 400). Thermal analyses were conducted for the as-made samples after washing with water and drying at 100 °C. The measurements were conducted in air flow (15 cm^3/min). They comprised TG and DTA measurements recorded with a Netzsch STA 449 apparatus on line with an HP 86B computer. Platinum crucibles contained about 100 mg of the sample. Calcined kaolin was used as reference material. The temperature rate in the range of 20–650 °C was 5 °C/min.

Considering a possible reduction of incorporated zinc in hydrogen atmosphere or with other reducing agents, we have also measured TPR data for selected samples. The TPR curves have been recorded with an Asap ChemSorb 2705 apparatus. The flow rate of hydrogen (10%)/argon mixture was 108 ml/min. The temperature increase (20–900 °C) was 10 °C/min. TPR measurement (Fig. 8) has been taken for zincosilicate (Zn/Si = 0.05) after template removal as well for its modification with copper cations. The Cu content was ≈0.6 wt.%. The samples were calcined at 400 °C in helium stream before the measurement.

TABLE I
Synthesis conditions

Sample	Molar ratios (gel)[a] Zn : Si : T : Na : A : H_2O	Crystallization time, h	Zn, ppm in the product	Zn/Si in the product	Product structure[b]
EZF01	0.01 : 1 : 0.08 : 0.24 : 0.03 : 20	23	1.260	0.00881	MFI
EZF02	0.02 : 1 : 0.08 : 0.48 : 0.06 : 20	23	2.045	0.0145	MFI
EZF03	0.03 : 1 : 0.08 : 0.72 : 0.09 : 20	23	2.492	0.0176	MFI
EZF04	0.04 : 1 : 0.08 : 0.92 : 0.12 : 20	69	2.756	0.0196	MFI
EZF05	0.05 : 1 : 0.08 : 1.00 : 0.15 : 20	115	2.989	0.0211	MFI
EZF06	0.06 : 1 : 0.08 : 1.20 : 0.18 : 20	93	[c]	[c]	MFI + Q + am
EZF07	0.07 : 1 : 0.08 : 1.30 : 0.21 : 20	46	[c]	[c]	MFI
EZF08	0.08 : 1 : 0.08 : 1.40 : 0.24 : 20	138	3.196	0.0228	U + Q + MFI
EZF09	0.09 : 1 : 0.08 : 1.50 : 0.27 : 20	111	[c]	[c]	MFI + U + Q + am
EZF10	0.10 : 1 : 0.08 : 1.60 : 0.30 : 20	93	[c]	[c]	MFI + Q + U + am

[a] T, template; A, H_3PO_4. [b] Q, quartz; U, unknown phase; am, amorphous material. [c] Not analyzed.

Catalytic activity of the samples was examined in propan-2-ol decomposition and in cumene cracking. The tests were conducted in a pulse microreactor combined with a gas chromatograph. The catalyst powder samples (15 mg) were activated in helium stream at 400 °C for 30 min prior to the catalytic tests. Cumene cracking was carried out at 350 °C, and decomposition of propan-2-ol at 200 °C with H-forms and at 250 °C with Cu-forms, respectively. The volume of injected substrate was 1 μl.

RESULTS AND DISCUSSION

As indicated in Fig. 1, zincosilicate samples with different zinc contents show a high crystallinity up to the Zn/Si ratio 0.07. There are no reflections that could be attributed to ZnO admixture. The higher zinc loading results in a noticeable contribution of quartz and amorphous phase in the products.

The scanning electron microscopic photographs (Fig. 2) show regular crystallites of the samples. The particle size depends on zinc loading decreasing with growing Zn content (3–10 μm).

The IR spectra show two bands in the range 1000–1100 cm^{-1} for the samples with low zinc loading, whereas the zinc-rich samples indicate only one band at 1050 cm^{-1} (Fig. 3a). The reported spectra of other metallosilicates[13] indicate the bands attributed to the Si–O–Me bonds. The bands are always observed at ≈900 cm^{-1}. If the stretching bands of lower wavenumbers (≈1020 cm^{-1}) were assigned to Zn–O it would be difficult to explain their absence in the Zn-rich samples. The spectrum of the sample modified

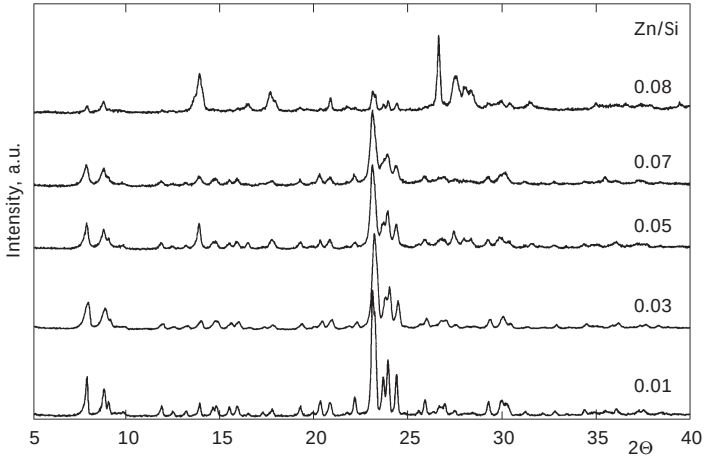

FIG. 1
XRD patterns of selected zincosilicate samples (Zn/Si indicated)

with NH_4 cations (Fig. 3b) clearly indicates the presence of N–H bands (1400 cm^{-1}), which proves the ion-exchange properties of the prepared zincosilicates. The ion-exchange ability results from the negative lattice charge caused by the introduced zinc tetrahedra. Our attempts to employ the Raman spectroscopy[23] indicated the presence of the band at ≈300 cm^{-1} in zincosilicate MFI, which is assigned to tetrahedral Zn [35]. Its intensity decreased on heating (Fig. 4), which indicates removal of some zinc from the lattice tetrahedral positions. The band at ≈380 cm^{-1} attributed to octahedral Zn became predominant after calcination. The solid state ^{29}Si MAS NMR data[29] indicate (Fig. 5) the predominant signal at ≈114 ppm, corresponding to silicon tetrahedron surrounded by four adjacent Si tetrahedra. Another

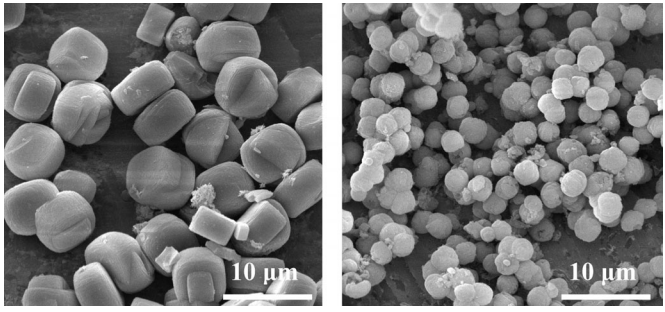

FIG. 2
Scanning electron micrograph of the samples with: a Zn/Si = 0.01 and b Zn/Si = 0.07

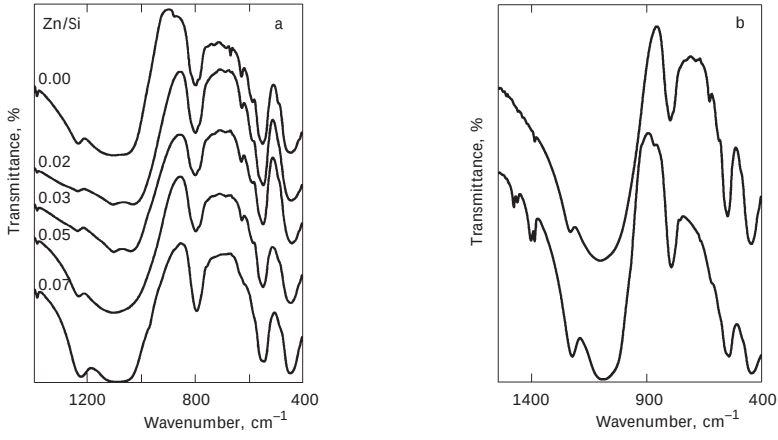

FIG. 3
IR spectra (KBr pellets) of the indicated samples (a), and of the sample with Zn/Si = 0.05 (b) (upper spectrum) and its ammonium modification (lower spectrum)

smaller signal at ≈103 ppm, results from silicon connected with three Si tetrahedra. The fourth adjacent neighbor is most likely the ZnO_4 unit. The intensity of the latter signal decreases markedly after calcination of the sample, which indicates that a part of zinc is released from the lattice positions (Fig. 5). However, the ability of the calcined samples to undergo the cation-exchange modification (Fig. 3) clearly indicates the presence of some zinc in the lattice.

Thermal analyses (Fig. 6) comprised both the zinc-free silicalite-1 and a series of MFI zincosilicates with various Zn contents (up to Si/Zn = 0.07). The thermal data are presented in Figs 6a–6c, where the samples of similar

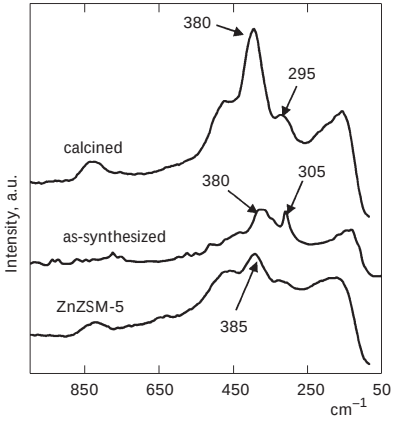

FIG. 4
Raman spectra of the indicated samples

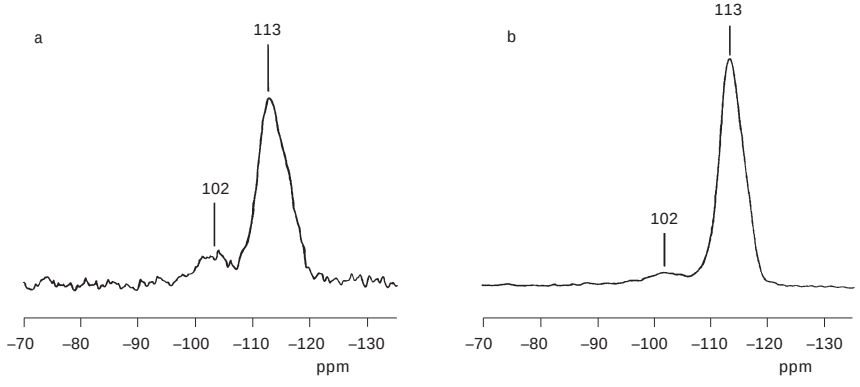

FIG. 5
^{29}Si MAS NMR spectra of the sample with Zn/Si = 0.05: a as-synthesized, b after calcination at 450 °C

thermal behavior are compiled. The weight loss for all the samples under study is ≈15%, regardless of the zinc loading. A contribution of water desorption (below 300 °C) is almost negligible (≈1%) for the silicalite and

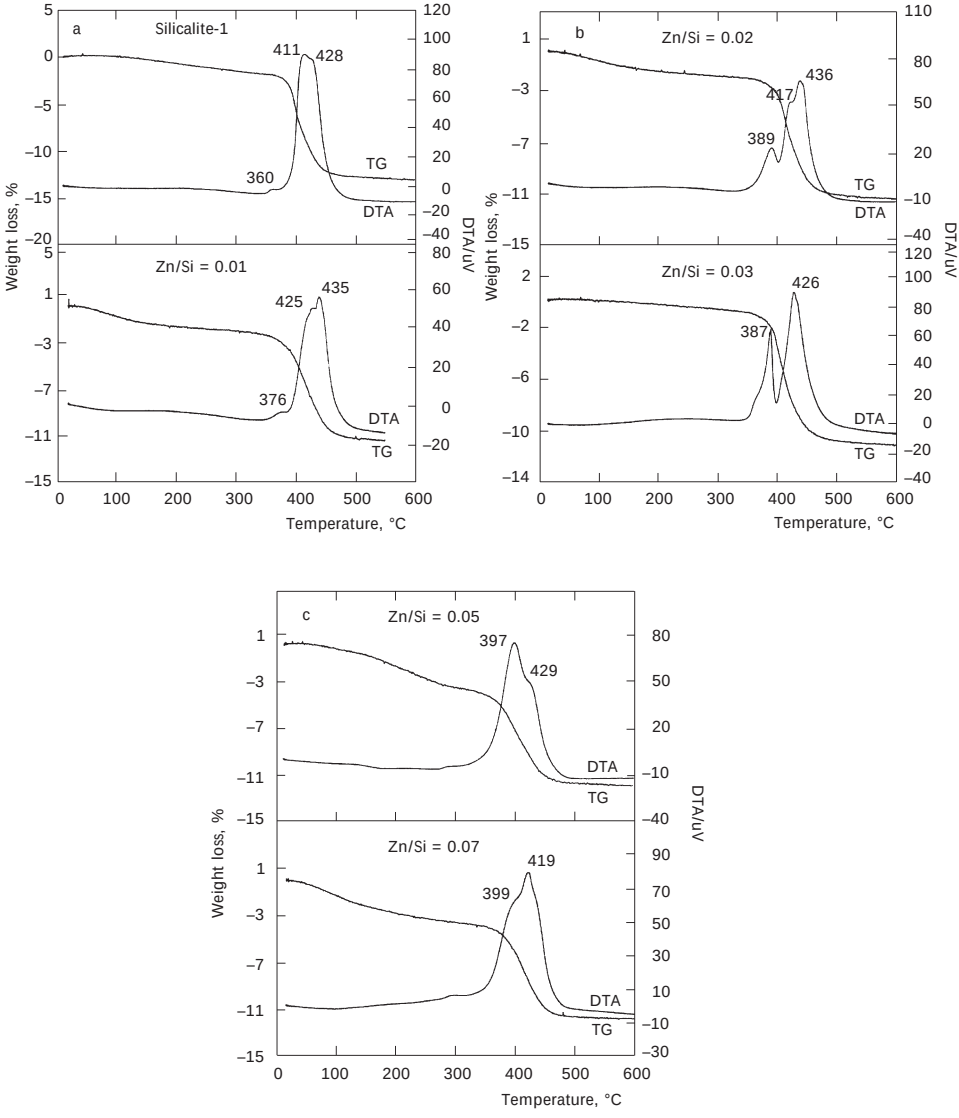

FIG. 6
Thermal analyses (TG and DTG) of the indicated samples

for the samples with the low Zn/Si ratios. It becomes more distinctive (≈5%) for the zinc-rich samples (Zn/Si = 0.05 and 0.07). The desorption of water proceeds gradually without any steps and no endothermic effect (DTA) accompanies this process. It is remarkable that none of the samples shows the thermal effect (up to 600 °C) which could be attributed to thermal decomposition of the crystalline structure. The XRD data of the samples calcined at 450 or 600 °C indicate well preserved crystalline structure. The DTA curves in Fig. 6a indicate small exothermic peaks in the range 360–375 °C and very large exothermic effects at *ca* 410–430 °C. The respective peaks for silicalite are at ≈20 °C lower temperature than that for zincosilicate (Zn/Si = 0.01). The exothermic effects result from the oxidative decomposition of organic template. A separation of these peaks could suggest different localization of removed organic additive (*i.e.* outer surface – below 400 °C and channel – above 400 °C). However, the DTG curves (not indicated in Fig. 6) do not exhibit two separated DTG peaks corresponding to withdrawal of template from different sites. The exothermic peaks below 400 °C become very distinctive for the samples with Zn/Si = 0.02 and 0.03 (Fig. 6b) and their intensities bring near that of exothermic effects above 400 °C. Again, only one DTG peak accompanies the exothermic effects. Thus, the valley between the exothermic peaks could be rather consider as the endothermic effect overlapping with the exothermic peak. In the case of the zinc rich samples (Zn/Si = 0.05 and 0.07) shown in Fig. 6c the exothermic effects above 400 °C are not separated. The correlation between the zinc content and the temperature of DTG peaks (Fig. 7) shows that temperature of tem-

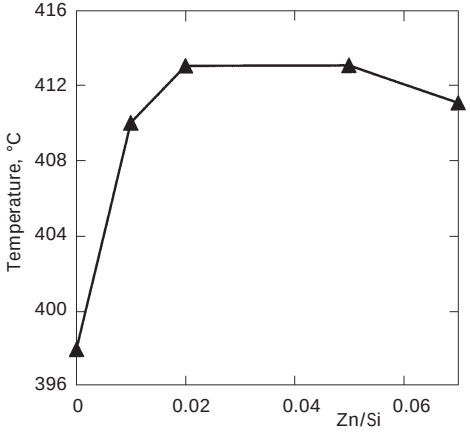

FIG. 7
Correlation between the Zn/Si ratio of the samples and temperature of the DTG peaks

plate removal is affected remarkably by the presence of zinc introduced into the MFI structure. An increase in the DTG temperature is particularly significant for the samples with the lowest zinc content. The increased temperature of template removal for the zincosilicates can result from stronger bonding of the TPA cations to the negatively charged lattice. Deeper interpretation of thermal results requires a further study. So far we can observe a distinctive difference in thermal behavior of the samples of low (up to Zn/Si = 0.03) and high zinc contents. This corroborates the observed differences in properties of the samples with low and high zinc content (catalytic activity, ion-exchange capacity[36]). The latter are probably less ordered and contain more structure defects.

The measurement of thermal-programmed reduction (TPR) in hydrogen indicates (Fig. 8) relatively high resistance of the zincosilicate of MFI structure to the reduction, regardless of relatively high zinc loading (Zn/Si = 0.05). Some consumption of hydrogen starts after exceeding the temperature of 500 °C. A small peak is noticeable at ≈580 °C and two distinct large reduction peaks are observed at temperatures 730 and 850 °C. The TPR profiles of the samples with lower Zn content do not differ very much from that indicated in the Fig. 8. The peak at 580 °C can be assigned to Zn cations[20] and we noticed that it is more pronounced for the sample modified with Zn cations. The other larger peaks result from the reduction of the lattice zinc. The modification of zincosilicate MFI with copper cations (0.6 wt.%) significantly affects the reducibility of the sample. The Cu^{2+} cations undergo the reduction already at ≈200 °C. The distinctive and large peak at-

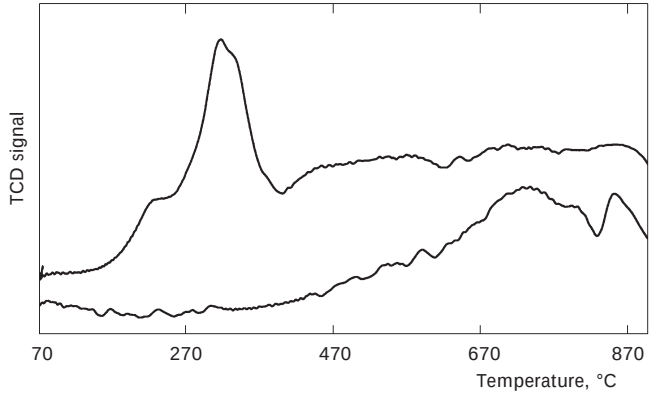

FIG. 8
TPR profiles for the sample with Zn/Si = 0.05 after template removal (lower curve) and for its Cu modification (upper curve)

tains the maximum at ≈320 °C. Further temperature rise does not result in very distinct peaks, although the consumption of hydrogen is considerable. This indicates that the lattice Zn is involved in the reduction. The peak attributed to the Zn cations is still noticeable, although shifted above 600 °C. The TPR curve declines above 900 °C, which can suggest that the zinc reduction is complete at this temperature. The shape of TPR profiles differs very much from those for silicalite impregnated with ZnO described by Wan[18], where the reduction of zinc oxide already started at 200 °C, as well as from zeolite MFI modified with Zn cations (introduced either by ion-exchange or impregnation), where the main TPR peak appeared at 550 °C [20].

The catalytic tests with the H-forms of MFI zincosilicates in cumene cracking indicate a noticeable activity of the samples (Fig. 9). The only products detected were benzene and propene. The introduction of zinc into the lattice results in appearance of strong-acid sites capable of initiating this reaction. The activity increases with the Zn content up to Zn/Si = 0.02 and 0.03. Further increase in the Zn content results in reduced activity. However, the activity of the series is distinctly lower than that of MFI (Al/Si = 100). The activity in propan-2-ol decomposition over the H-forms of the samples under study is also most pronounced for the samples with low zinc loading (Fig. 10) and the correlation between the zinc loading and catalytic activity reminds that for cumene cracking. The dehydration is the only reaction route. The distinctively lower activity of zinc-rich samples results from less ordered structure of the latter. It seems, however, that acid sites present in the zinc-rich samples are relatively strong despite their limited

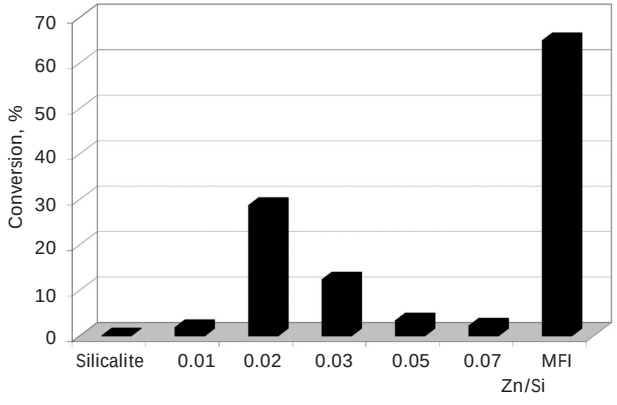

FIG. 9

Conversion of cumene as a function of the Zn/Si ratio in H-forms of zincosilicalite used as catalysts. The conversion over MFI is included for comparison

number, since they show some activity in cumene cracking. The samples modified with Cu^{2+} cations (Fig. 11) showed much lower activity in propan-2-ol decomposition than the H-forms and, therefore, the test was conducted at higher temperature. The correlation between the zinc concentration and the activity is quite different than for H-forms. The introduction of the least amount of Zn (Zn/Si = 0.01) manifests itself in the highest activity. Further increase in the Zn content results in an activity decrease. The influence of the copper introduced on the selectivity of the reaction is very significant. The contribution of dehydrogenation to acetone becomes

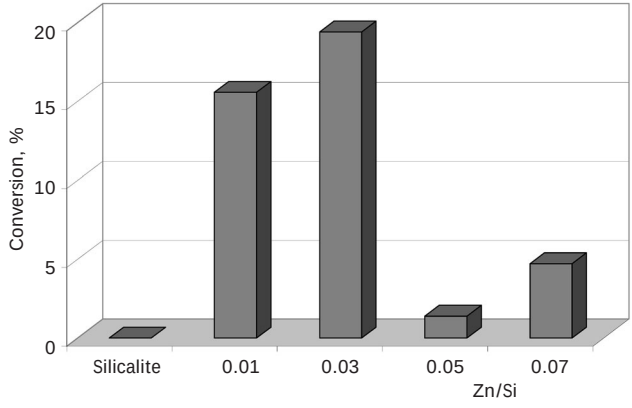

FIG. 10
Conversion of propan-2-ol (at 200 °C) as a function of the Zn/Si ratio in H-forms of zincosilicalites used as catalysts

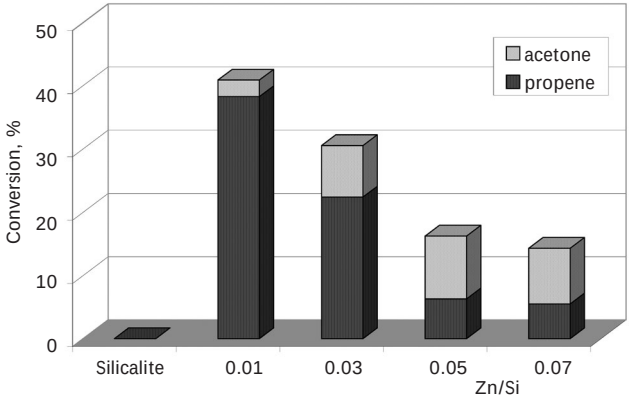

FIG. 11
Conversion of propan-2-ol over Cu-forms of the samples (at 250 °C) as a function of the Zn/Si ratio, contributions of acetone and propene are indicated

very remarkable. The acetone content increases with the zinc loading attaining more than 50% of the product mixture for the Zn-rich samples (Fig. 11).

CONCLUSIONS

Zinc can be introduced into the MFI structure by conventional hydrothermal synthesis. The presence of phosphate anions in the initial mixtures is advantageous. The resulting MFI zincosilicates show high crystallinity of Zn/Si ratios below 0.07. Further increase in the Zn content results in formation of amorphous products or nonporous crystalline phase (quartz). The crystallization time depends on the zinc content and a higher Zn loading requires a longer crystallization. The properties of the resulting samples are distinctively affected by introduced "heteroatoms". There are considerable differences in properties of the samples with low zinc contents (up to Zn/Si = 0.03) and those exceeding this ratio. Thermal analyses of the as-synthesized products show similar curves for the samples with low Zn contents (up to Zn/Si = 0.03). The introduction of Zn into the lattice results in enhanced temperature of template removal, compared with zinc-free silicalite. The negative lattice charge of zincosilicates results in stronger interaction with the TPA cations and increases thermal stability of the latter. The thermal analyses do not indicate the thermal structure degradation up to 600 °C which is consistent with XRD data. The ^{29}Si MAS NMR spectra of zincosilicates under study indicate the signal at ≈102 ppm, which results from silicon surrounded by three Si and one Zn tetrahedra. The intensity of the above signal declines on heating because of a removal of some Zn from the lattice. The Raman spectra also exhibit the band (≈300 cm^{-1}), which could be assigned to the tertahedral lattice Zn. The intensity of this band decreases after thermal treatment, because some of the Zn atoms are release from the lattice. Regardless of that the calcined samples can be modified with various cations. The TPR measurement indicates quite high resistance of zincosilicate to reduction with hydrogen (up to ≈600 °C). The possibility of modifying the obtained zincosilicates by ion-exchange and their noticeable catalytic activity (contrary to the zinc-free silicalite-1) in cumene cracking and in propan-2-ol decomposition strongly supports the localization of the introduced zinc in the lattice. The acid site strength in H-modifications of zincosilicates is much lower than that in H-ZSM-5, but the modification of these materials with transition metal cations (*e.g.* Cu) could be promising in the red-ox reactions.

S. Kowalak and E. Szymkowiak-Janiszewska appreciate financial support of the Polish Committee of Scientific Research (KBN) (grant No. 1249/T09/2001/20).

REFERENCES

1. Gier T. E., Stucky G. D.: *Nature* **1991**, *349*, 508.
2. Harrison W. T. A., Gier T. E., Morgan K., Nicol J., Eckert H., Stucky G. D.: *J. Am. Chem. Soc.* **1991**, *3*, 27.
3. Harrison W. T. A., Nenoff T. M., Gier T. E., Stucky G. D.: *J. Solid State Chem.* **1994**, *113*, 168.
4. Nenoff T. M., Harrison W. T. A., Gier T. E., Stucky G. D.: *J. Am. Chem. Soc.* **1991**, *113*, 378.
5. Novak-Tusar N., Kaucic V.: *Zeolites* **1995**, *15*, 708.
6. Kumar N., Lindfors L.-E.: *Stud. Surf. Sci. Catal.* **1995**, *94*, 325.
7. Kumar N., Lindfors L.-E., Byggningsbacka R.: *Proc. 8th Int. Symp. Heterogeneous Catal., Varna 1996*, p. 249, (A. Andreev, L. Petrov, Ch. Bonev, G. Kadinov, I. Mitov, Eds). Institute of Catalysis, Bulgarian Academy of Sciences, Sofia 1996.
8. Annen M. J., Davis M. E., Higgins J. B., Schlenker L.: *J. Chem. Soc., Chem. Commun.* **1991**, 1175.
9. Camblor M. A., Davis M. E.: *J. Phys. Chem.* **1994**, *98*, 13151.
10. Freyhardt C. C., Lobo R. F., Khodabandeh S., Lewis J. E., Jr., Tsapatsis M., Yoshikawa M., Camblor M. A., Pan M., Helmkamp M. M., Zones S. I., Davis M. E.: *J. Am. Chem. Soc.* **1996**, *118*, 7299.
11. Röhring C., Gies H.: *Angew. Chem., Int. Ed. Engl.* **1995**, *34*, 63.
12. Valange S., Gabelica Z., Onida B., Garrone E.: *12th International Zeolite Conference, Baltimore 1999* (Mater. Res. Soc.), p. 2711, (M. M. J. Treacy, B. K. Marcus, M. E. Bisher, J. B. Higgins, Eds). Warrendale, Pennsylvania 1999.
13. Szostak R.: *Molecular Sieves – Principles of Synthesis and Modification*. Van Nostrand Reinhold, New York 1989.
14. Kowalak S., Jankowska A., Baran E.: *Chem. Commun.* **2001**, 575.
15. Ono Y.: *Catal. Rev.–Sci. Eng.* **1992**, *87*, 179.
16. Roessner F., Hagen A., Mroczek U., Karge H. G., Steinberg K.-H.: *Stud. Surf. Sci. Catal.* **1993**, *75*, 1707.
17. Skrzypek J., Słoczyński J., Ledakowicz S.: *Methanol Synthesis*. Polish Scientific Publishers, Warszawa 1994.
18. Wan B.-Z., Min Chu H.: *J. Chem. Soc., Faraday Trans.* **1992**, *88*, 2943.
19. Berndt H., Lietz G., Luecke B., Voelter J.: *Appl. Catal., A* **1996**, *146*, 351.
20. Berndt H., Lietz G., Voelter J.: *Appl. Catal., A* **1996**, *146*, 365.
21. Inui T., Makino Y., Okazumi F., Miamoto A.: *Stud. Surf. Sci. Catal.* **1988**, *37*, 487.
22. Kowalak S., Szymkowiak E., Giordano G.: *Europa-Cat-IV, Rimini 1999*. Book of Abstracts, p. 849. European Federation of Catalysis Societies, 1999.
23. Kowalak S., Szymkowiak E., Jankowska A., Giordano G.: *Proc. 9th Int. Symp. Heterogeneous Catal., Varna 2000*, p. 229, (L. Petrov, Ch. Bonev, G. Kadinov, Eds). Institute of Catalysis, Bulgarian Academy of Sciences, Sofia 2000.
24. Kowalak S., Szymkowiak E., Lehmann I., Giordano G.: *Stud. Surf. Sci. Catal.* **2001**, *135*, 311.

25. Giordano G., Katović A., Szymkowiak E., Kowalak S.: *ZMPC 2000*, p. 106. Sendai, Japan 2000.
26. Robson H. (Ed.): *Verified Syntheses of Zeolitic Materials*. Elsevier, Amsterdam 2001.
27. Kumar R., Bhaumik A., Ahedi R. K., Ganapathy S.: *Nature* **1996**, *381*, 298.
28. Nagy J. B., Bodart P., Hannus I., Kirici I.: *Synthesis, Characterization and Use of Zeolitic Microporous Materials*. Deca Gen Ltd., Szeged (Hungary) 1998.
29. Katovic A., Szymkowiak E., Giordano G., Kowalak S., Fonseca A., Nagy J. B.: *Stud. Surf. Sci. Catal.* **2001**, *135*, 337.
30. Parker E. L. M., Bibby D. M., Patterson J. E.: *Zeolites* **1984**, *4*, 168.
31. Soulard M., Bilger S., Kessler H., Guth J. L.: *Zeolites* **1987**, *7*, 463.
32. Gabelica Z., Nagy J. B., Bodart P., Dewaele N., Nastro A.: *Zeolites* **1987**, *7*, 67.
33. Crea F., Giordano G., Mostowicz R., Nastro A.: *Therm. Anal.* **1990**, *36*, 2229.
34. Nastro A., Nagy J. B., Crea F., Lee J. C., Hayhurst D. T., Giordano G.: *Thermochim. Acta* **1988**, *135*, 403.
35. Rudolph W. W., Pye C. C.: *Phys. Chem. Chem. Phys.* **1999**, *1*, 4583.
36. Kowalak S., Szymkowiak E.: Unpublished results.